Hindawi
Modelling and Simulation in Engineering
Volume 2019, Article ID 3467050, 18 pages
https://doi.org/10.1155/2019/3467050

Research Article

Combined DFT and Fuzzy Based Faulty Phase Selection and Classification in a Series Compensated Transmission Line

Praveen Kumar Mishra and Anamika Yadav

Department of Electrical Engineering, National Institute of Technology, Raipur 492010, India

Correspondence should be addressed to Anamika Yadav; ayadav.ele@nitrr.ac.in

Received 31 August 2018; Accepted 14 January 2019; Published 3 February 2019

Academic Editor: Jing-song Hong

The conventional distance protection scheme malfunctions sometimes in case of a fixed series capacitor compensated transmission line due to the change in relaying impedance of the protected line during faulty conditions. In order to mitigate this problem, a combined discrete Fourier transform and fuzzy (CDFTF) based algorithm has been proposed in this paper. This method has been tested on a 400 km, 735 kV series compensated transmission line network and WSCC 3-machine 9-bus system for all fault types using MATLAB/Simulink and PSCAD platforms, respectively. A fixed series capacitor is located at the middle of the protected line. The fundamental components of phase currents, phase voltages, and zero-sequence current are fed as inputs to the proposed scheme. The fault detection, faulty phase selection, and fault classification are achieved within 1/2–1 cycle of power frequency. The proposed CDFTF-based scheme is less complex and is better than other data mining techniques which require huge training and testing time. Test results corroborate the proposed scheme reliability with wide variations in fault location, fault resistance, fault inception angle, evolving faults, compensation level, and heavy load interconnection. The results discussed in this work indicate that the proposed technique is resilient to wide variations in fault and system conditions.

1. Introduction

The primary reasons behind adoption of a series capacitor in the long transmission line include increased transmittable power, improved transient stability, voltage stability, power oscillation damping, and thereby reduced transmission and revenue losses. When the power system is subjected to a short circuit fault, it is accompanied by flow of huge fault current which may damage of the connected equipments and also create power quality problems. Therefore, accurate fault detection and classification are very crucial tasks in power system protection to restore the power supply and to improve the reliability. The installation cost of SCs is also less for 15–30% compensation as compared to installation/erection of a new line, and also it is not affected by environmental concerns [1, 2]. Distance relays used for the protection of a fixed series compensated line may experience overreach during a fault due to the involvement of the series capacitor in the fault loop, and also the distance function may fail to pick up a low fault current in the protected line. The distance relay protects 80–85% of the transmission line length, and it operates based on the impedance seen by relay location. The inclusion of a capacitor in the line either compensates or cancels a part of the transmission line inductance, which may result in a fault seen by the relay in its 1st zone although the fault has actually occurred in the 2nd or 3rd zone of protection. Similarly, a fault in the 1st zone can be perceived to be a fault in the reverse direction. For proper isolation of the faulty phase(s), correct knowledge of the faulted phase(s) is essential. Fast and reliable fault detection and classification technique is an important requirement in power transmission systems to maintain continuous power flow [3]. If the transmission line is series compensated, this task becomes more complicated.

Various schemes have been proposed earlier for fault classification in uncompensated and compensated transmission lines. These algorithms usually require measurements at one end or two ends of lines. To complement the

existing methods, a sequence component-based method is proposed in [4]. In [5], decision tree-based fault classification is proposed for a transmission line compensated by a fixed series capacitor. Phase selection based on superimposed voltages and currents under balanced load is proposed in [6]. Faulty phase selection based on an integrated moving sum approach is proposed for SCTS in [7]. The authors of [8, 9] have developed fault classification algorithms using artificial neural networks (ANNs), but sometimes ANN-based approaches are subjected to underfit and overfit problems and may also stuck in a local minima. Methods based on adaptive neurofuzzy (ANFIS) for fault classification in the long transmission line have been proposed in [10, 11]. In [12–14], a support vector machine (SVM) has been used to classify the fault, but the schemes based on machine learning techniques require huge computational burden and are quite complex. In [15–18], fault classification schemes based on fuzzy logic have been presented with different feature extraction techniques such as discrete Fourier transform [15], wavelet transform [16], higher order statistics [17], and angular differences among the sequence components of the fundamental currents [18]. Fault classification technique based on probabilistic neural networks (PNNs) is discussed in [19]. In [20], the authors have conferred the effectiveness of an extreme learning machine for the protection of a long transmission line. Cross-country faults and evolving faults have been investigated in [21]. Furthermore, hyperbolic S-transform and support vector regression method have been developed for protection of series compensated lines in [22]. In [23], an intelligent relaying scheme based on decision tree (DT) has been validated in the real-time digital simulator (RTDS). Recently, discrete wavelet transform and k-nearest neighbour have been used for fault detection, classification, and location estimation in a double circuit series compensated line in [24].

The main challenges in fault classification in an extra-high-voltage (EHV) series compensated transmission line are as follows:

(a) The conventional distance relay employed in an EHV transmission line may mal-operate during stressed conditions such as load variation, power swing, load encroachment, and system frequency variation. Also the distance relay underreaches and overreaches during high-resistance fault and fault with high DC offset current.

(b) Series capacitor is a popular device to increase the current carrying capacity of a transmission line by reducing the effective length of line. Change in the line current and voltage affects the seen impedance by the conventional distance relay. Moreover, it may result in voltage or current inversion and hence result in malfunction of the relay for certain types of faults [2].

(c) Moreover, it is required to have two separate algorithms to deal with faults occurring before series capacitor and after series capacitor.

(d) Presence of a metal oxide varistor (MOV) and bypass switches may also lead to the challenges [2] in protection of transmission lines. MOVs change the effective impedance of the installation depending on the degree of MOV conduction, which is nonlinear.

This paper aims to validate the CDFTF-based approach for classification of all the shunt faults in a series compensated system. Feasibility of the proposed CDFTF-based scheme has been tested on a 735 kV, 60 Hz, and 400 km long transmission system and a modified WSCC 3-machine 9-bus system which is a midpoint-fixed series capacitor compensated in MATLAB/Simulink [25]and EMTDC/PSCAD platforms, respectively. The main novelty of the proposed work can be explained as follows:

(a) The proposed scheme is very simple and easy to implement as it uses the fundamental phasor of the signals at one end only and then it applies the Fuzzy approach to make the final decision.

(b) In the proposed scheme, one single Fuzzy-based relay can detect and classify the fault either before or after the series capacitor, whereas in the existing scheme two separate algorithms are required.

(c) There is no requirement of a communication channel between two ends and hence the reliability is improved, and furthermore cost and computation burden is reduced.

(d) The speed of the presented relaying scheme is within half cycle of power frequency (i.e., less than 10 ms).

(e) The proposed scheme works well for an evolving fault and heavy load interconnection.

(f) Efficacy of the proposed scheme is also validated on a modified WSCC 3-machine 9-bus series compensated network and provides an average accuracy of 99.678%.

The paper is divided into six sections. Section 2 gives a brief overview of the series compensated transmission system. In section 3, the CDFTF-based scheme is discussed. In section 4, it illustrates the performance of the proposed algorithm under different fault scenarios. In section 5, it compares the proposed with earlier reported schemes. In the final section, the concluding remarks have been given.

2. Series Compensated Transmission System (SCTS)

The single-line diagram of 735 kV, 60 Hz SCTS is shown in Figure 1. It consists of a doubly-fed series compensated transmission system wherein source 1 is a power plant consisting of six 350 MVA generators and source 2 is a Thevenin equivalent source of the interconnected grid. The line 1 between bus B3 and bus B2 has 100 km length while the line between bus B4 and B2 has 300 km length. Further to enhance the power transmission capability of the system, the 300 km line 2 between buses B4 and B2 is the midpoint compensated by a fixed series capacitor of 62.8 μF in each

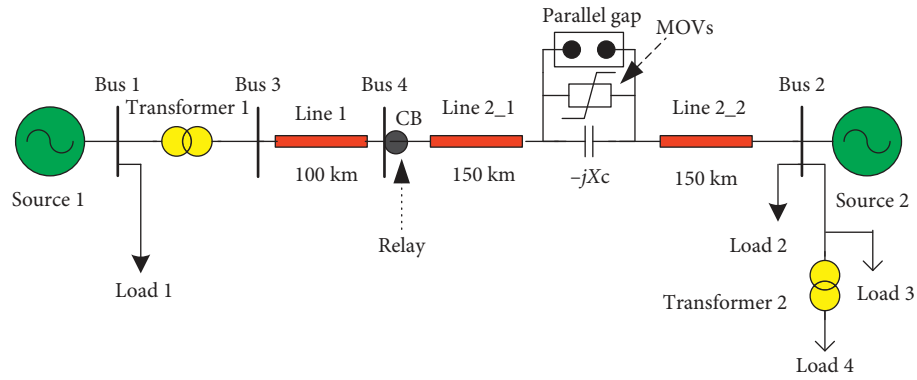

Figure 1: Single-line diagram of a series compensated power system network.

phase representing 40% compensation of the reactance of line 2.

The SC is protected by the MOV block which consists of 60 columns, and its protection level is set to 238.9 kV. This voltage corresponds to 2.5 times the nominal capacitor voltage. All fault simulation studies have been carried out using the MATLAB/Simulink platform [25]. SC is protected by MOV overvoltage and the air gap. For simulation studies, a sampling frequency of 1.2 kHz is chosen. Figure 1 shows a schematic diagram of the simulated system. The system parameters are given in Appendix A.

3. Proposed CDFTF-Based Fault Classification Scheme

In this work, combined DFT and fuzzy logic technique based on the fault classification scheme has been proposed for a series compensated transmission system. Figure 2 presents the flow chart of the proposed CDFTF-based technique. The fundamental component magnitude of 3-phase voltages and currents are obtained after preprocessing the single-end measurements. In the preprocessing stage, the 3-phase time domain (instantaneous) voltage and current signals are converted into discrete samples through zero-order hold block with a sampling frequency of 1.2 kHz and passed through a 2nd-order low pass Butterworth filter with a band pass edge frequency of 2 ∗ pi ∗ 400 rad/s. Furthermore, the filtered discrete 3-phase signals are passed through the recursive discrete Fourier transform (DFT) block available in MATLAB/Simulink to obtain the fundamental components of voltages and currents in the time domain. For knowledge of the ground involvement in the fault, a sequence analyzer is used to calculate the magnitude of zero-sequence current.

After preprocessing, the fundamental component magnitude of 3-phase currents and voltage signals are applied to the proposed fuzzy-based fault classification algorithm. Fuzzy logic is an extension of multivalued logic and problem solution methodology which gives a better and precise conclusion from vague and imprecise data. Basically, fuzzy logic has four stages: (i) fuzzification; (ii) inference system; (iii) fuzzy rule base/knowledge base; and (iv) defuzzification. In fuzzification, crisp inputs are converted into fuzzified inputs, which are processed by the inference system according to the rules defined in the rule base/knowledge base. The decision taken by the inference system is fuzzy in nature which cannot be understood by the real-time system, so this is mapped into crisp output through the defuzzification stage. The membership function shape is very important with respect to the performance of the whole system. In this work, the triangular membership functions for fuzzification and the centroid method for defuzzification have been chosen. Figure 2 presents the flow chart of the proposed CDFTF-based technique.

During the fault in the forward direction, only fuzzy-based fault classifier is activated which determines the types of faults along with the phase(s) involved. Inputs for the FFC are the magnitudes of fundamental voltage and current. The fuzzy based fault classifier (FFC) is designed separately for each phase and also for ground identification.

Based on the type of fault that has occurred in the line, corresponding faulted phase(s) and ground output become high (1) and healthy phase(s) output remains low (1). Thus, both the faulty phase(s) and the type of fault are identified using the proposed scheme as exemplified in Figure 2. About the ground involvement, the magnitude of zero-sequence current is taken. For identification and classification of faulty phase(s), the fundamental component of voltage and current using DFT is considered as input. The zero-sequence current signal is obtained using the sequence analyzer in order to determine the ground involvement.

Steps to design the fuzzy rules are as follows:

(a) Simulate all ten types of faults in the MATLAB/Simulink model of the test system at 10 km and 290 km from the relaying bus with the variation in fault resistance (i.e., 10 Ω and 100 Ω) and fault inception angle (0, 45, 90, and 270).

(b) Obtain the fundamental components of voltage and current signals using the full-cycle DFT algorithm and also estimate the zero-sequence current signal.

(c) After observing the behaviour of voltage and current signals for all simulated cases as discussed in step (a), categorize the voltage and current signals into three ranges such as V_{LOW}, V_{MED}, and V_{HIGH} and I_{LOW}, I_{MED}, and I_{HIGH}, respectively. And also to know the ground involvement in fault conditions,

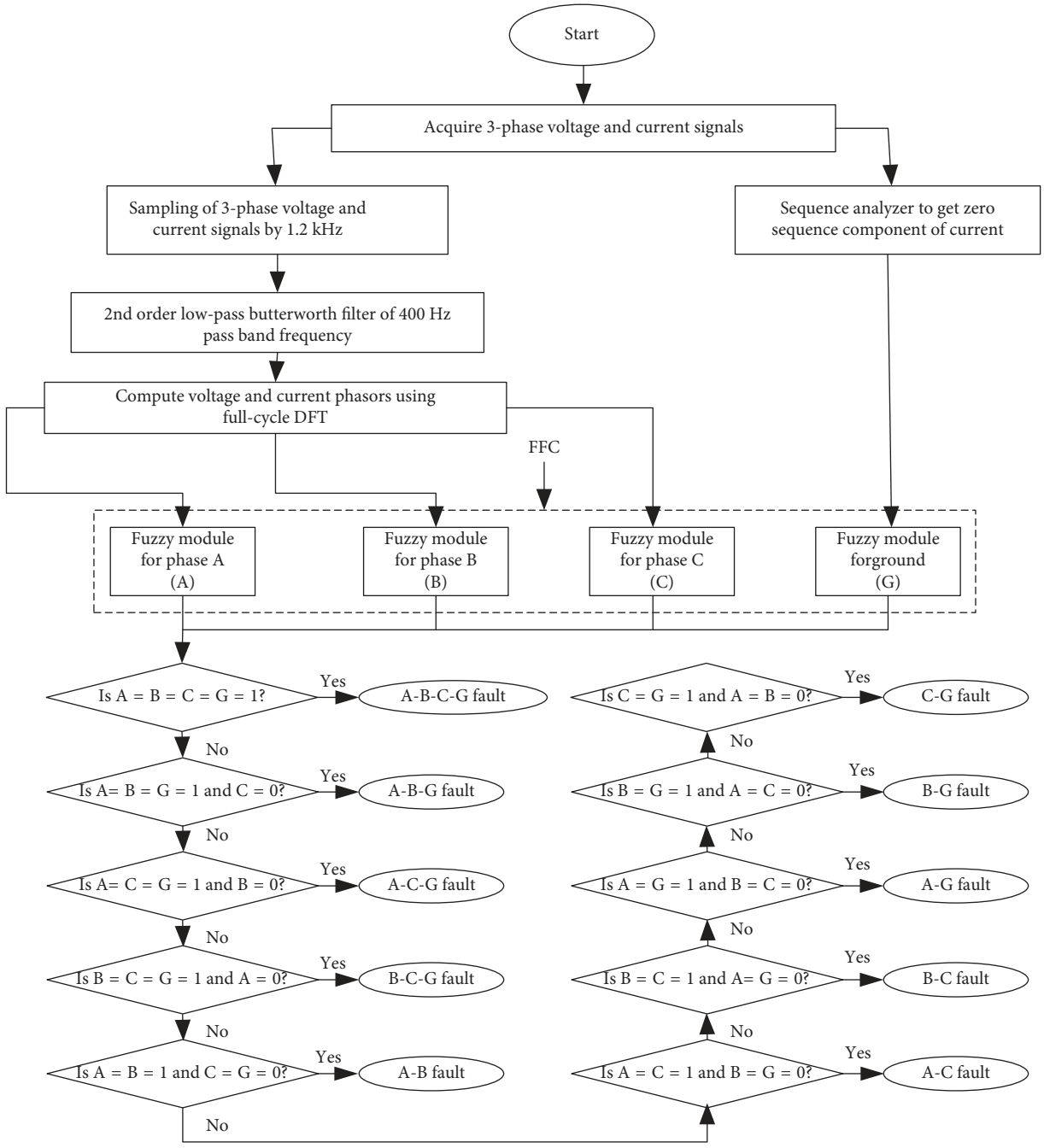

Figure 2: Flow chart of the proposed CDFTF-based scheme.

subcategorize zero-sequence current into the three ranges I_{LOW}, I_{MED}, and I_{HIGH}.

(d) Design the fuzzy rule base and ranges of membership functions as depicted in Tables 1 and 2.

Each voltage and current signal is divided into three ranges with triangular membership function (TMF): low, medium, and high, as described in Table 2. FFC provides four outputs corresponding to the three phases, namely, "phase A," "phase B," "phase C," and "ground G" which goes high (1) in the case of fault occurrence or else remains low (0) during healthy conditions. Output trip logic also consists of two ranges, namely, trip low TL (0) and trip high TH (1). The effect of variations on different fault factors has also been studied, such as fault type, fault location, fault resistance, fault inception angle, evolving fault, compensation level, etc.

Table 1: Fuzzy rule base for fuzzy-based faulty phase classification.

Parameter	I_{LOW}	I_{MID}	I_{HIGH}
V_{LOW}	TL	TH	TH
V_{MID}	TL	TH	TH
V_{HIGH}	TL	TH	TH

Table 2: Membership function.

	Quantity	P	Q	R
Phase classification	V_{LOW}	0	2×10^5	3×10^5
	V_{MID}	2×10^5	3×10^5	5×10^5
	V_{HIGH}	3×10^5	5×10^5	1×10^6
	I_{LOW}	0	1000	2000
	I_{MID}	1000	2000	3000
	I_{HIGH}	2000	3000	15000
Ground detection	I_{LOW}	0	30	60
	I_{MID}	30	60	200
	I_{HIGH}	60	200	2000

As illustrated in Figure 2, if a fault occurs in the protected zone, three-phase voltage and current signals are acquired at the relay point which will be further preprocessed by full-cycle DFT for the feature extraction process. The sampling frequency for the collected signal is kept to be 1.2 kHz. To know the ground involvement, the zero-sequence component of the current signal has been calculated. Extracted features of voltage and current signals, i.e., fundamental components, are fed to the fuzzy module of phase(s). FFC deliver the four outputs A, B, C, and G which are declared as "zero" in the case of "no fault" and otherwise "one."

If A = B = C = G = 1, then FT is ABCG fault; if A = B = G = 1 and C = 0, then FT is ABG fault; if A = B = 1 and C = G = 0, then FT is AB fault; if A = G = 1 and B = C = 0, then FT is AG fault.

In this paper, we have used TMF as shown in Figure 3 which is specified by three parameters {P, Q, R} whose values have been taken as described in Table 2 for phase(s) as well as for ground detection and classification. The rule base designed for ground detection is as follows:

(i) If zero-sequence current is I_{LOW} or I_{MID}, then the trip is TL

(ii) If zero-sequence current is I_{HIGH}, then the trip is TH

Detection and classification time of the relay for faulty phase(s) can be calculated as follows:

$$T_r = T_o - T_i, \quad (1)$$

where T_r, T_o, and T_i stand for the response time taken by the relay to classify the faults, the relay operating time, and the time of inception of a fault, respectively. From Table 3, it is clear that the time taken to classify phase(s) and ground is less than half cycle in almost all of the fault cases. The SCTS has been simulated using MATLAB/Simulink software.

The aim of this study is to validate various fault circumstances, and a huge fault dataset has been considered with wide variations in fault parameters, such as fault location (FL), fault resistance (FR), fault inception angle (FIA), and fault type (FT) under wide variations in system conditions. The different system conditions have been generated with various compensation levels. The values of the fault parameters considered in this paper are as follows:

(i) Fault location (FL): 20 number of random locations

(ii) Fault resistance (FR): 0.001, 10, 20, 30, 40, 50, 60, 80, and 100 Ω

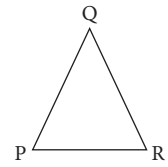

Figure 3: Triangular membership.

(iii) Fault inception angle (FIA): 0°, 45°, 90°, 135°, 180°, 225°, 270°, 315°, and 360°

(iv) Fault type (FT): all 10 types (LG, LLG, LL, and LLL)

(v) Level of compensation (%X): uncompensated, 10, 20, 30, 40, 50, 60, and 65% for FIA = 0°

Therefore, a total of 129600 fault cases has been generated [(FL ∗ 20) ∗ (FR ∗ 9) ∗ (FIA ∗ 9) ∗ (FT ∗ 10) ∗ (%Xc ∗ 8)].

4. Performance Evaluation of the Proposed Scheme

To evaluate the effectiveness of the CDFTF-based scheme, a 735 kV, 60 Hz 3-phase series compensated transmission system (SCTS) with a distributed line model as shown in Figure 1 has been considered and simulated in the MATLAB/Simulink environment. The system details have been provided in Appendix A. During normal system condition, power flow takes place from Bus B1-B2. The voltage and current signals are acquired at the relaying point, i.e., at Bus B4. The sampling rate for the collection of voltage and current signals is maintained at 1.2 kHz.

4.1. Effect of Fault Location. The effect of variations in the fault location on the performance of the presented scheme has been analyzed with varying resistance in the range of 0.001 Ω to 50 Ω for all shunt faults. Test results of the variations in fault locations are summarized in Table 4. Figures 4(a) and 4(b) show the time domain signals of 3-phase voltage and current during the AB fault occurred at 135 km from the relaying point with FR = 10 Ω, FIA = 0° at 0.5 sec. Figure 4(c) shows the performance of the classification module in which phases A and B rise up (1) both at 0.5042 sec. Phase C and ground G remain low (0) after the inception of the fault at 0.5 sec. So, the proposed scheme provides better protection, covering 90% of the line length.

Table 3: Faulty phase detection and fault classification using FFC with variations in fault parameters.

Simulated system data			Results obtained from the proposed CDFTF-based scheme				
			Response time (ms)				
FL (km)	FR (ohm)	FIA (degree)	Phase A	Phase B	Phase C	Ground G	Fault type
30	100	90	—	—	4.133	3.334	CG
60	0.001	135	6.25	4.55	—	2.85	ABG
90	10	180	—	4.167	9.967	4.167	BCG
120	100	0	5.8	—	8.3	3.3	CAG
149	0.001	45	3.717	10.417	5.417	—	ABC
180	10	90	8.333	9.133	—	—	AB
210	100	135	—	5.35	9.55	—	BC
240	0.001	180	7.467	—	7.467	—	CA
270	10	0	5.8	—	—	5	AG

Table 4: Effect of fault location (FIA = 0°).

Simulated system data			Results obtained from the proposed CDFTF-based scheme				
			Response time (ms)				
Fault type	FL (km)	FR (ohm)	Phase A	Phase B	Phase C	Ground G	Fault type
AB	10	10	4.10	3.30	—	—	AB
AB	135	10	4.10	4.10	—	—	AB
AB	175	10	5.80	12.50	—	—	AB
ABG	10	50	5.00	3.30	—	3.30	ABG
ABG	95	50	5.00	4.10	—	4.10	ABG
ABC	10	10	4.10	3.30	7.50	—	ABC
ABC	95	10	5.00	3.30	8.30	—	ABC
ABC	120	10	5.00	3.30	9.10	—	ABC

4.2. Effect of Fault Resistance. Another parameter that might have an impact on fault classification is fault resistance because, in the case of faults involving ground, FR may cause incorrect operation of the conventional distance relay. The impacts of this parameter on the proposed scheme have been studied with variations in fault resistance. Test results during variations of FR on the presented CDFTF-based technique are shown in Table 5. The proposed method has been proved to be effective in classifying the fault type with variations in fault resistance ranging from 0.001 Ω to 100 Ω. Figures 5(a) and 5(b) show the input to FFC 3-phase time domain voltage and current signals. Figure 5(c) presents the performance of FFC output. In Figure 5, LLG (ABG)-type fault occurred in protected SCTS with FR = 40 Ω and FIA = 45° at FL = 205 km is shown. The output of FFC shows that phases A and B and ground G go high (1) at 0.5067 sec, 0.5108 sec, and 0.5083 sec, respectively, after the inception of the fault at 0.5025 sec with phase C remaining low (0) and unchanged, confirming the nature of ABG fault. Table 5 summarizes the performance of the proposed scheme, which presents the time required to classify the fault(s) that is considerably less than half cycle of power frequency in most of the cases.

4.3. Effect of Fault Inception Angle. Faults in a transmission line can occur at any time instant. So, the proposed CDFTF-based method has also been tested for varying FIA, and results have been presented in Table 6. For all the tested cases, the response time for classification of faults is within one cycle of power frequency in most of the cases. Fault classification inputs and outputs during ABC-type LLL fault including FIA = 180° at 175 km from the relaying point are shown in Figure 6. 3-phase sinusoidal voltages and currents are shown in Figures 6(a) and 6(b), respectively. Figure 6(c) shows the outputs of FFC where all the three faulty phases A, B, and C become high (1) after 0.5167 sec and ground output G remains low (0) all the time.

4.4. Effect of Fault Type. The proposed CDFTF-based method also helps in identifying and classifying the faulty phase(s) with the variation in shunt fault types. Basically, there are 10 fault types that involve all combinations of A, B, C, and G. All FT must be applied to test the ability of the relay for accurate classification of the faulty phase(s). Some of the results are tabulated in Table 7. The response time of the presented CDFTF-based relay with wide variations in fault types is included in Table 7.

Figures 7(a) and 7(b) show the graphical time domain 3-phase voltage and current signals at relaying bus B4 for an AG fault including FIA = 45° and FR = 50 Ω at 50 km. Figure 7(c) shows the output of FFC in which phase A and ground G go high (1) at 0.5058 sec and 0.5050 sec, respectively, and all other phases remain low (0), clearly indicating the occurrence of AG fault. Hence, it can be inferred that the proposed technique is capable of classifying faults in less than half cycle in most of the cases.

4.5. Effect of Evolving Faults. The effectiveness of the proposed CDFTF-based technique has been examined for

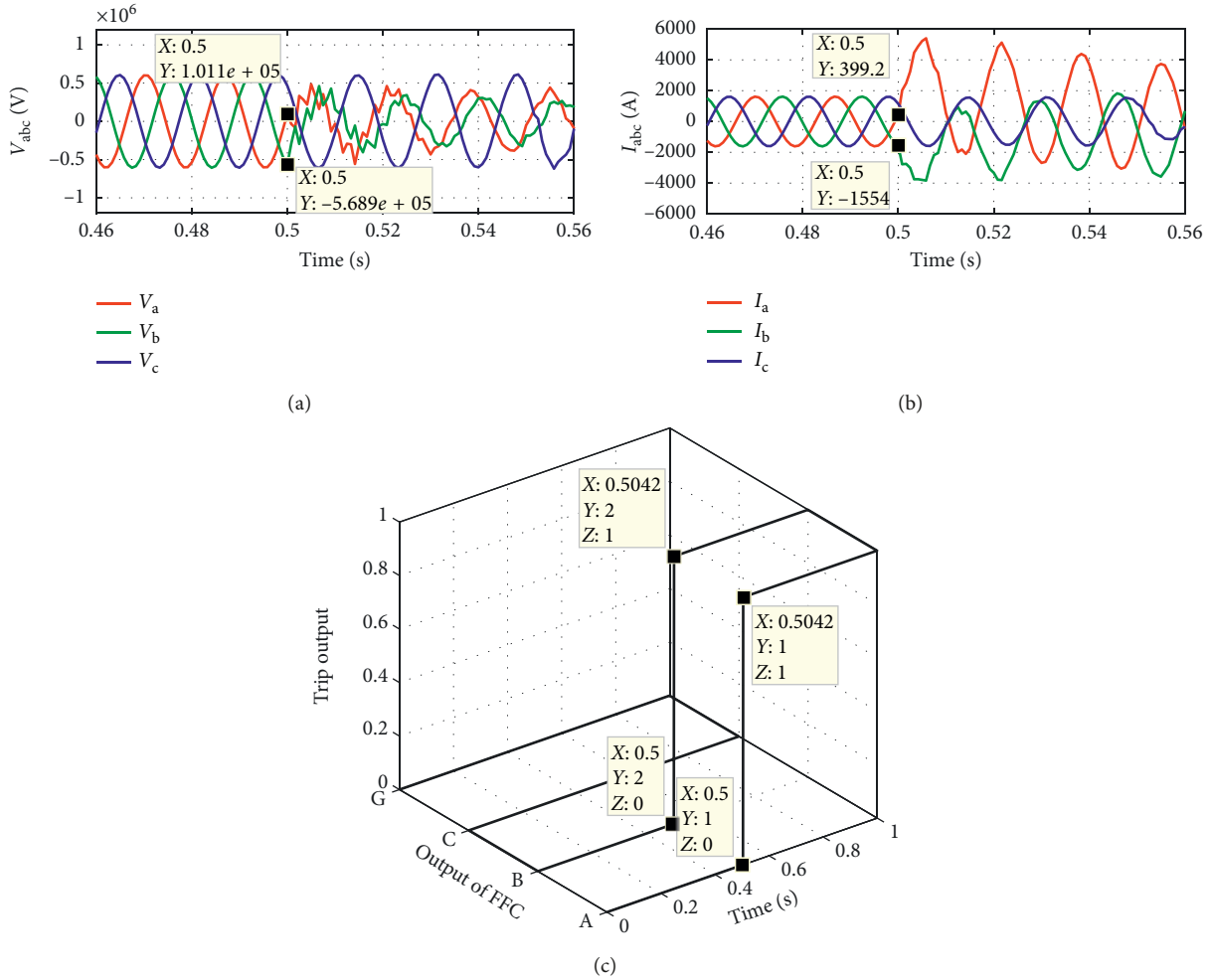

FIGURE 4: Performance during AB fault at 135 km, FIA = 0°, and FR = 10 Ω: (a) 3-phase voltage waveform; (b) 3-phase current waveform; (c) output of FFC.

TABLE 5: Effect of fault resistance (FIA = 45°).

Simulated system data			Results obtained from the proposed CDFTF-based scheme				
			Response time (ms)				
Fault type	FL (km)	FR (ohm)	Phase A	Phase B	Phase C	Ground G	Fault type
ABG	25	0.001	3.717	4.517	—	4.517	ABG
ABG	55	20	3.717	4.517	—	4.517	ABG
ABG	95	80	4.517	9.517	—	5.417	ABG
ABG	175	20	3.717	9.517	—	5.417	ABG
ABG	205	40	4.1	8.3	—	5.8	ABG
ABG	245	100	6.217	9.517	—	7.017	ABG

evolving faults. An evolving fault can be defined as a fault where the involvement of phases changes over a period of time. For example, an evolving fault begins as a single line-to-ground fault, and after a short time interval, it transforms into a double line-to-ground fault [21]. The characteristic of an evolving fault is that its faulted phases change over time, while other types of faults' faulted phases remain unchanged. The effectiveness of the presented scheme during evolving faults has been examined, and some of the results are presented in Table 8. From Table 8, it can prove that the proposed CDFTF-based method can classify the evolving faults correctly within half cycle in most of the conditions. Figures 8(a) and 8(b) present the three-phase time domain voltage and current signal, and the output of FFC is presented in Figure 8(c). Single line to ground (BG) has been considered initially with FR of 15 Ω and fault inception time being 0.51 sec at 90 km from relaying bus B4. This BG fault is transformed into double line-to-ground fault (BCG) with FR

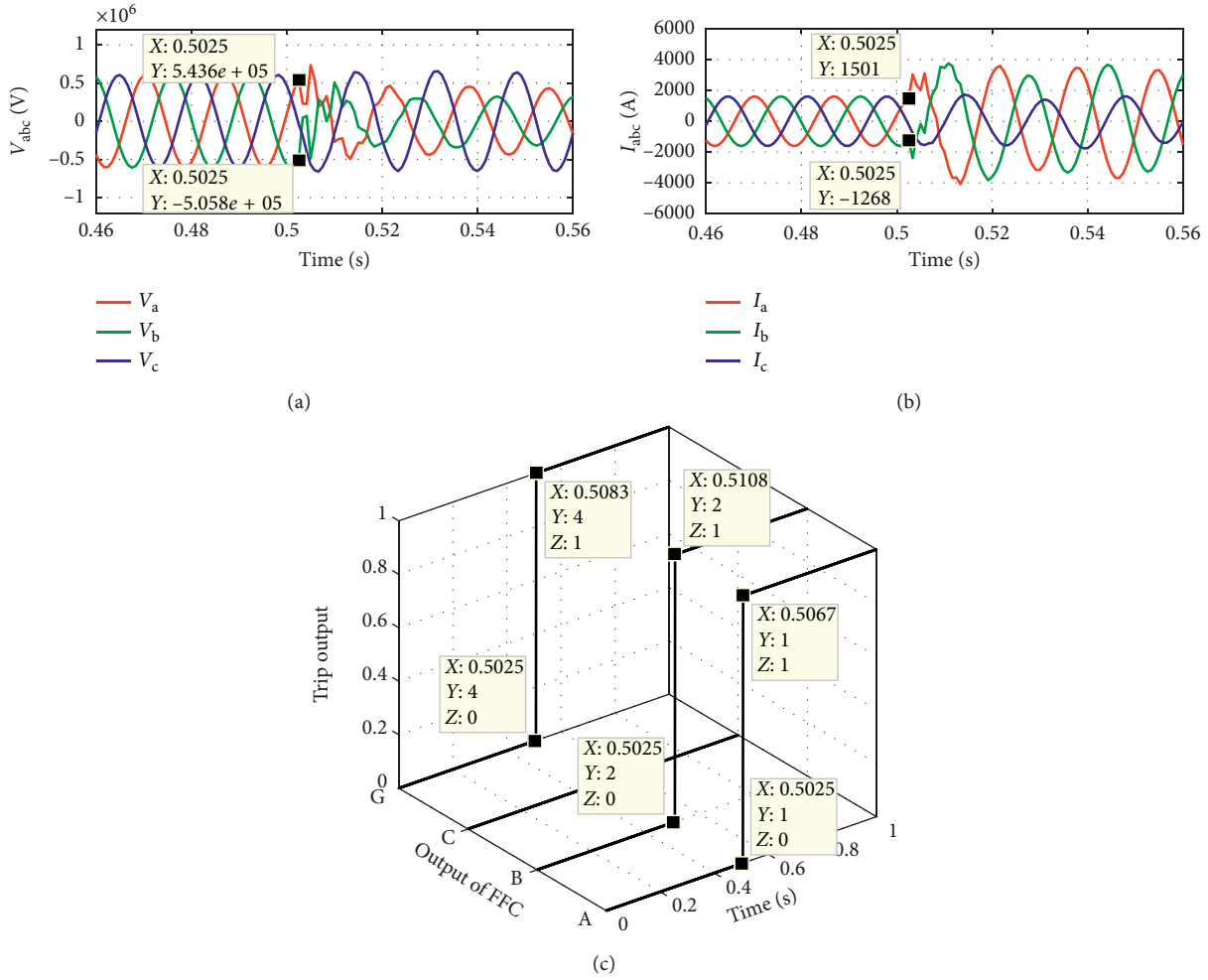

Figure 5: Performance during ABG fault at 205 km, FIA = 45°, and FR = 40 Ω: (a) 3-phase voltage waveform; (b) 3-phase current waveform; (c) output of FFC.

Table 6: Effect of FIA (FR = 50 Ω).

Simulated system data			Results obtained from the proposed CDFTF-based scheme				
Fault type	FL (km)	FIA (degree)	Response time (ms)				Fault type
			Phase A	Phase B	Phase C	Ground G	
ABG	55	45	3.717	22.91	—	2.917	ABG
ABG	95	90	9.9335	23.334	—	3.334	ABG
BCG	135	135	—	4.5503	4.5503	7.05	BCG
BCG	25	180	—	3.267	3.267	4.167	BCG
BC	175	315	—	4.518	4.518	—	BC
ABC	175	180	5.00	4.20	8.30	—	ABC

of 50 Ω just after the initiation of an initial fault. The time deviations between the two faults are 26 ms. In Figure 8(c), it is clearly examined that the faulty phases B and C and ground G become high (1) after fault inception with phase A remaining low (0). Proposed schemes correctly classify the faulty phase(s) within a cycle.

4.6. Effect of Level of Compensation. Most of the schemes which have been reported in the literature are basically designed for a specific compensation level; as the compensation level increases or decreases, the performance of schemes may get affected, and also at higher compensation levels, the SSR (subsynchronous resonance) phenomenon is predominant. To know the feasibility of the proposed scheme with the wide variations in the level of compensation level (from %Xc = 10%–80%), various simulation studies have been performed. Table 9 summarizes the results of the simulation studies.

The 3-phase voltage and current signals are shown in Figures 9(a) and 9(b) for a DLGF (double line-to-ground

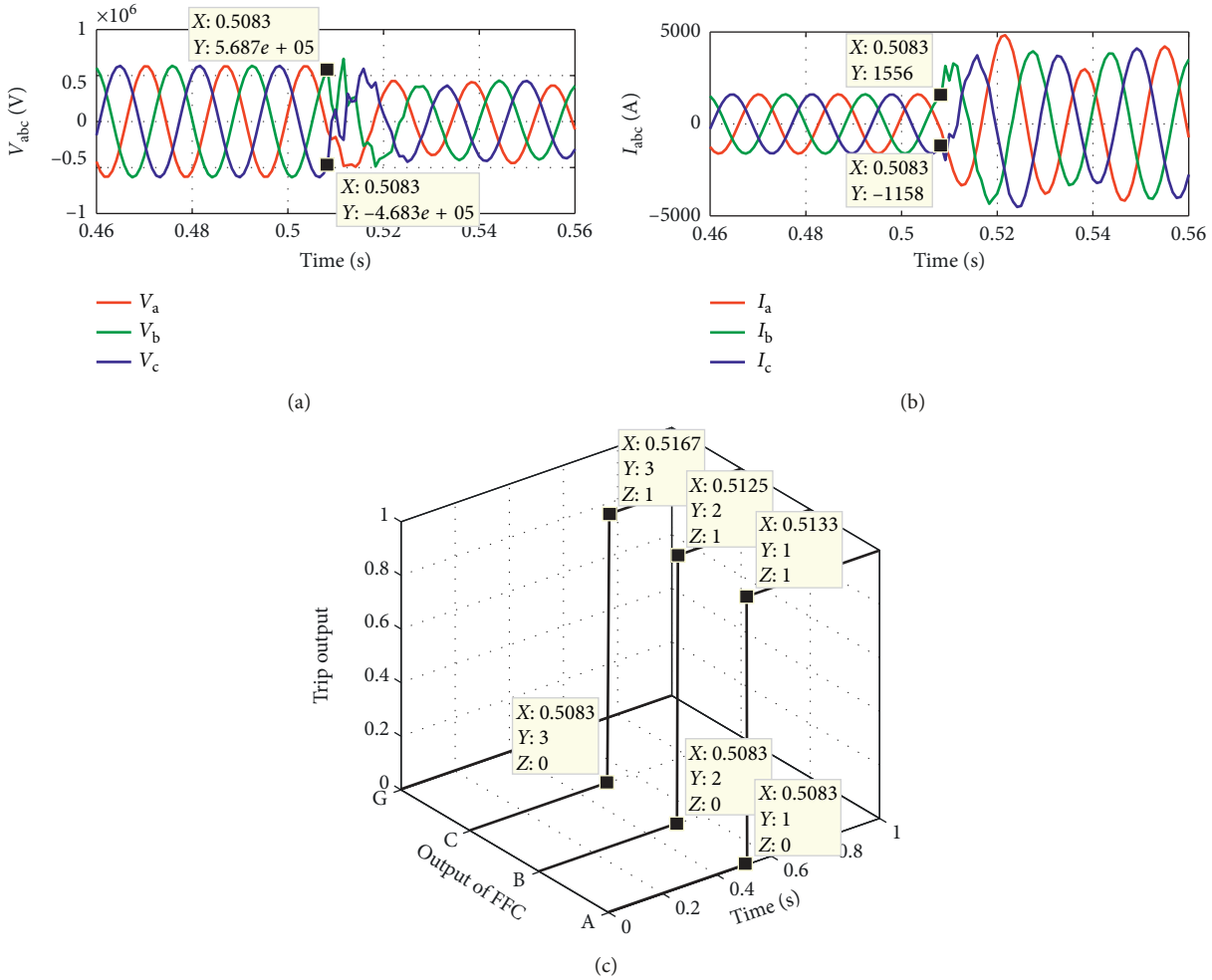

FIGURE 6: Performance during ABC fault at 175 km, FIA = 180°, and FR = 50 Ω: (a) 3-phase voltage waveform; (b) 3-phase current waveform; (c) output of FFC.

TABLE 7: Effect of fault type (FR = 50 Ω and FIA = 45°).

Simulated system data		Results obtained from the proposed CDFTF-based scheme				
Fault type	FL (km)	Response time (ms)				Fault type
		Phase A	Phase B	Phase C	Ground G	
AG	50	3.30	—	—	2.50	AG
BG	160	—	8.717	—	4.517	BG
CG	250	—	—	7.017	6.217	CG
ABG	50	3.717	8.717	—	4.517	ABG
BCG	160	—	8.717	6.217	4.517	BCG
CAG	250	5.417	—	6.217	4.517	CAG
AB	50	3.717	11.217	—	—	AB
BC	160	—	7.917	7.917	—	BC
CA	135	6.217	—	6.217	—	CA
ABC	245	4.517	8.717	7.017	—	ABC

fault) in phases B and C with an FR of 10 Ω and FIA of 0° at 165 km from relaying bus B4. The outputs of the fault classification network are shown in Figure 9(c), wherein phases B and C and ground (G) become high (1) after 3.3 ms, with phase A remaining low (0) all the time.

The results approve the accurate effectiveness of the proposed technique under wide variations in the compensation level. The proposed scheme gives a good result for the classification of faults and faulty phase(s).

4.7. Effect of Change in System Frequency. In the literature survey, we found that authors have not been discussed the performance of their schemes under wide variations in

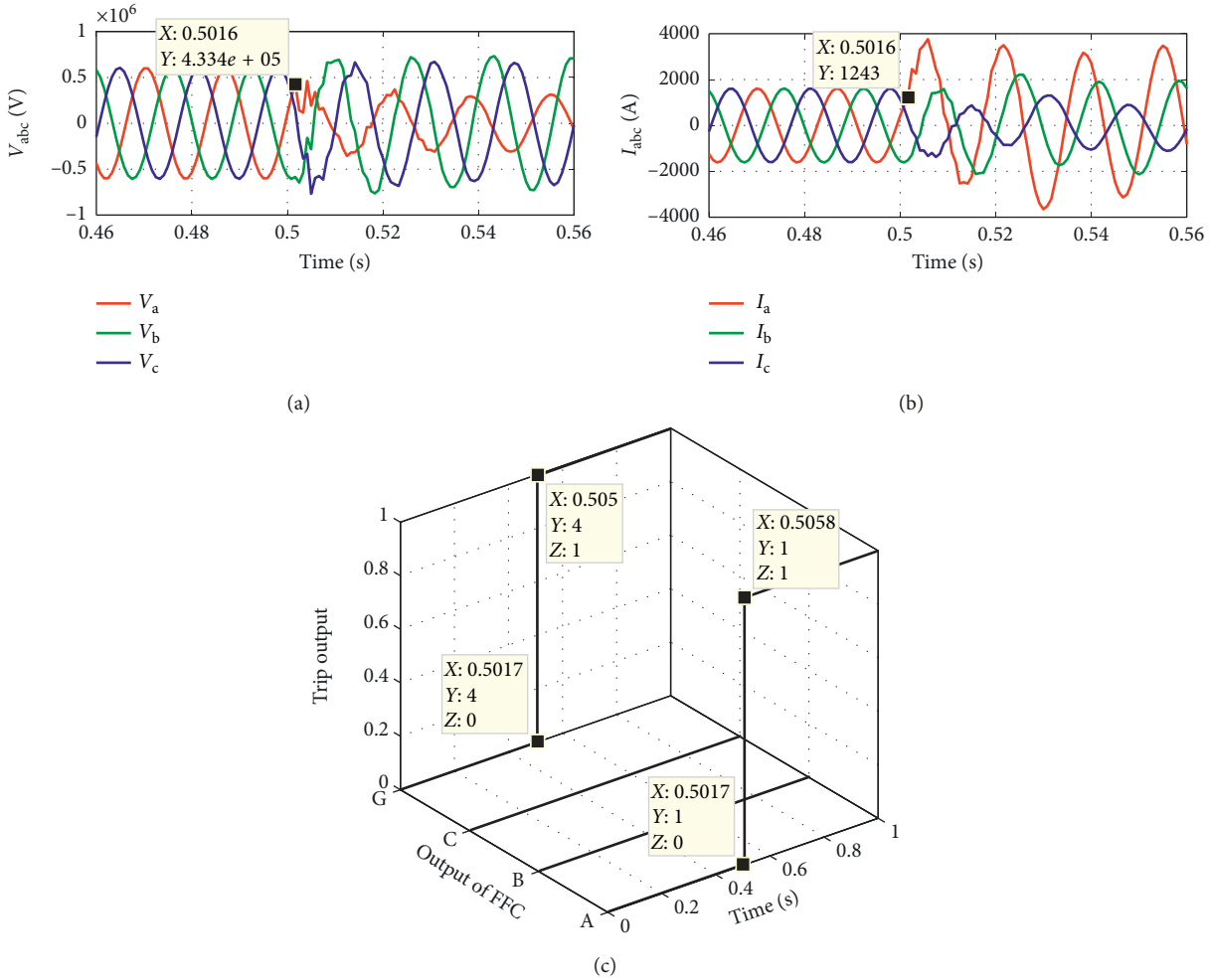

Figure 7: Performance during AG fault at 50 km, FIA = 45°, and FR = 50 Ω: (a) 3-phase voltage waveform; (b) 3-phase current waveform; (c) output of FFC.

Table 8: Simulation results for evolving faults.

Simulated system data								Results obtained from the proposed CDFTF-based scheme			
								Response time (ms)			
FT1	FT2	FR1 (Ω)	FR2 (Ω)	FL (km)	IT1 (s)	IT2 (s)	Time interval between IT1 and IT2 (ms)	Phase A	Phase B	Phase C	Ground G
AG	AG	10	5	50	0.5000	0.5150	15	5.00	—	—	3.30
AG	ABG	10	20	100	0.5025	0.5125	10	4.10	6.60	—	2.50
AG	ABCG	20	50	160	0.5016	0.5276	26	5.00	8.20	5.70	3.40
BG	BCG	15	50	90	0.5100	0.5360	26	—	10.80	4.80	3.30
BG	ABCG	5	30	250	0.5158	0.5258	10	5.00	5.00	8.30	4.20
AB	ABG	50	50	10	0.5025	0.5105	8	4.10	10.80	—	4.50
BC	ABC	1	30	80	0.5058	0.5288	17	4.50	4.20	4.20	—
BC	BCG	30	50	200	0.5200	0.5370	17	—	6.60	6.60	3.80
BC	ABC	50	1	175	0.5016	0.5316	30	6.70	8.40	8.40	—

FT1, initial fault types; FT2, secondary fault types; FR1, initial fault resistance; FR2, secondary fault resistance; IT1, inception time for the initial fault type; IT2, inception time for the secondary fault type.

system frequency. System frequency matters a lot in the protection of an electrical power system network. Various power system components such as induction machine, transformers, generators, and their operations depend on the frequency of the electrical system. Also, the stability of the power system relies on the frequency of the system. If

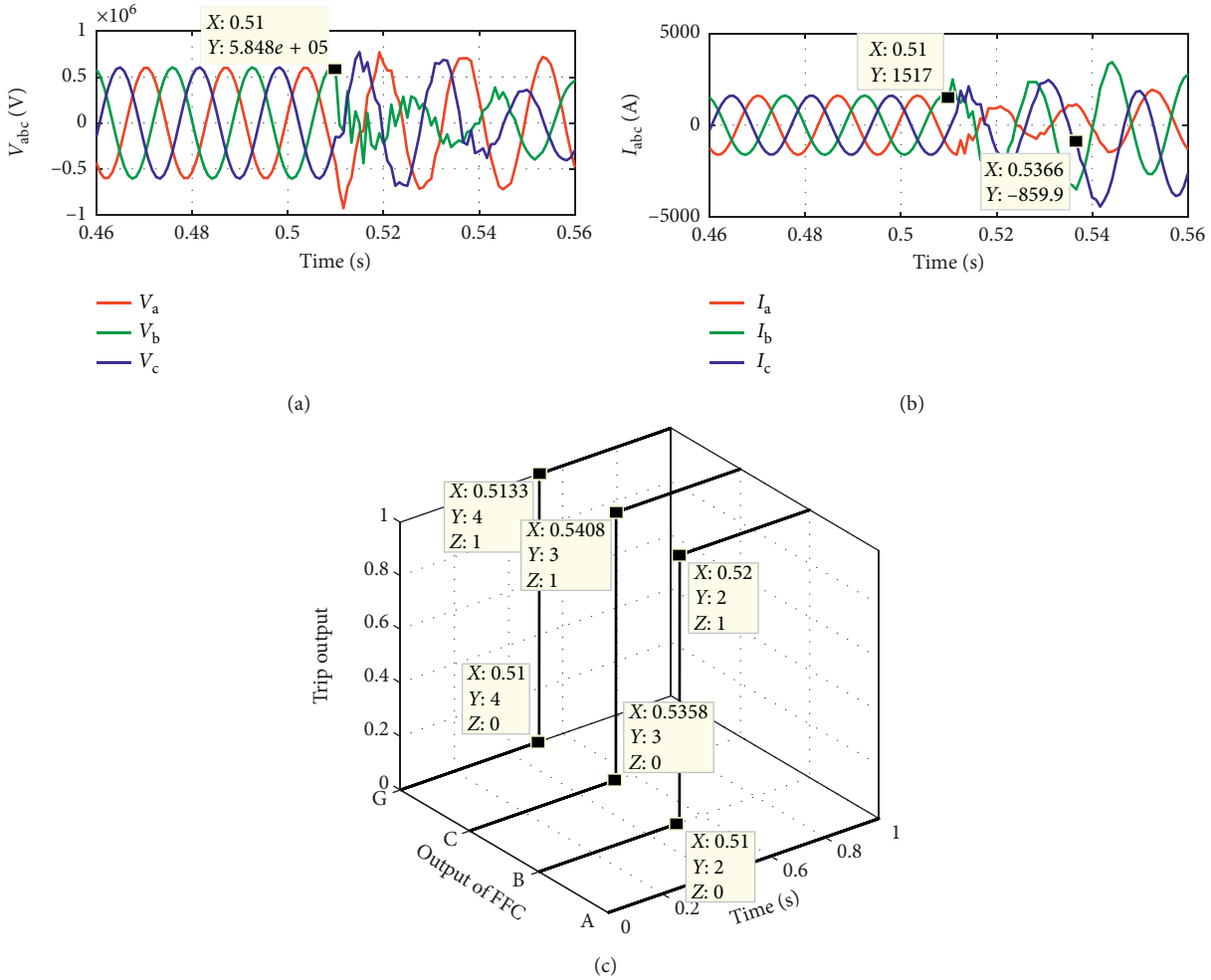

FIGURE 8: Performance during evolving fault case BG to BCG fault at 90 km, FR1 = 15 Ω, and FR2 = 50 Ω: (a) 3-phase voltage waveform; (b) 3-phase current waveform; (c) output of FFC.

TABLE 9: Simulation results for different compensation levels (BCG fault, FR = 10 Ω, and FL = 165 km).

Simulated system data			Results obtained from the proposed CDFTF-based scheme				
			Response time (ms)				
Fault type	%*Xc*	FIA (degree)	Phase A	Phase B	Phase C	Ground G	Fault type
BCG	Without capacitor	0	—	5.0	10.8	5.0	BCG
BCG	10	0	—	5.0	10.8	5.0	BCG
BCG	20	0	—	5.0	10.0	5.0	BCG
BCG	30	0	—	4.1	10.0	5.0	BCG
BCG	50	0	—	3.3	8.3	4.1	BCG
BCG	60	0	—	3.3	4.1	4.1	BCG
BCG	65	0	—	2.5	2.5	4.1	BCG

frequency deviation between the source end and the load end is more, then there is a probability of generators falling out of synchronism. To test the feasibility of the proposed method for the change in system frequency, consider fault type is DLGF in phases A and B with FR of 20 Ω and FIA of 0° at 170 km from relaying point B4 with wide variations in system frequency. Results are illustrated in Table 10.

Consider fault type is a double line-to-ground fault in phases A and B with an FR of 20 Ω and FIA of 0° at 170 km from relaying bus B4. The behaviour of voltage, current, and the proposed scheme during the ABG fault is shown in Figure 10.

Figure 10(c) shows that the outputs of the fault classification network wherein phases A and B and ground G become high after 4.2 ms, 3.5 ms, and 6.4 ms respectively,

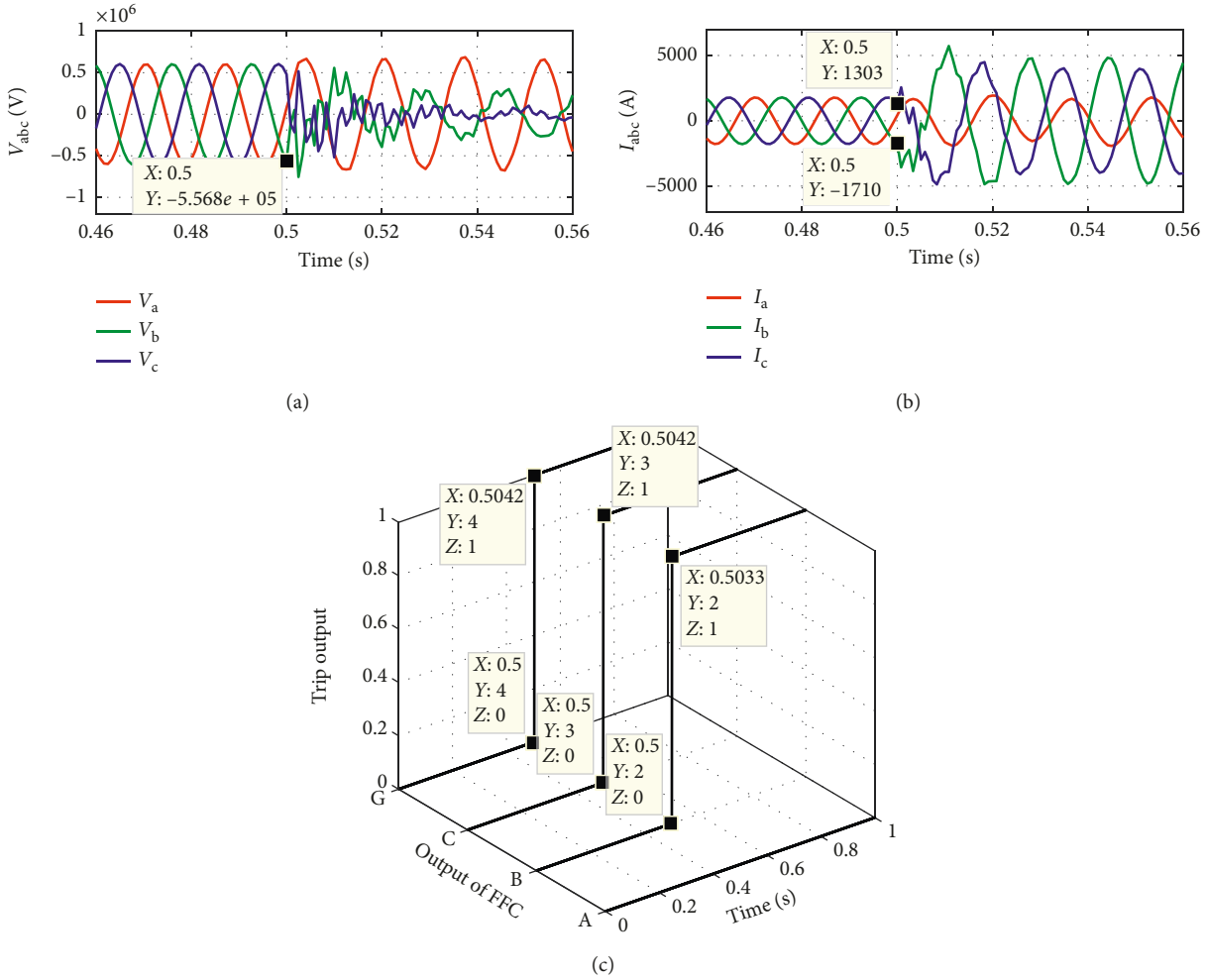

Figure 9: Performance during BCG fault at 165 km, FIA = 0°, FR = 50 Ω, and %Xc = 60%: (a) 3-phase voltage waveform; (b) 3-phase current waveform; (c) output of FFC.

Table 10: Simulation results for the wide variations in system frequencies (FIA = 0° and FL = 170 km).

Simulated system data			Results obtained from the proposed CDFTF-based scheme				
Fault type	FR (ohm)	System frequency (Hz)	Response time (ms)				Fault type
			Phase A	Phase B	Phase C	Ground G	
ABG		58	4.1	3.3	—	6.7	ABG
ABG		59	4.1	3.4	—	6.6	ABG
ABG	20	60	4.2	3.5	—	6.5	ABG
ABG		61	4.2	3.5	—	6.4	ABG
ABG		62	4.3	3.6	—	6.4	ABG

and phase C is low all the time. Results approve the accurate performance of the proposed method under wide variations in system frequency. The proposed scheme gives a good result for the classification of fault and faulty phase(s) within 7 ms.

4.8. Effect of Heavy Load Interconnection. Performance of the presented CDFTF-based technique has also been investigated for heavy load condition. Nature of the load is probabilistic in the distribution side. Sometimes, the relay considers sudden change in the load on bus as a fault. The relay may mal-operate, and the healthy part of the system might be removed, which creates nonreliability of power and causes revenue losses. In order to investigate the effect of heavy load interconnection on the effectiveness of the proposed scheme, a variety of simulations has been carried out, considering wide variations in system frequency. Some of the simulation results are presented in Table 11.

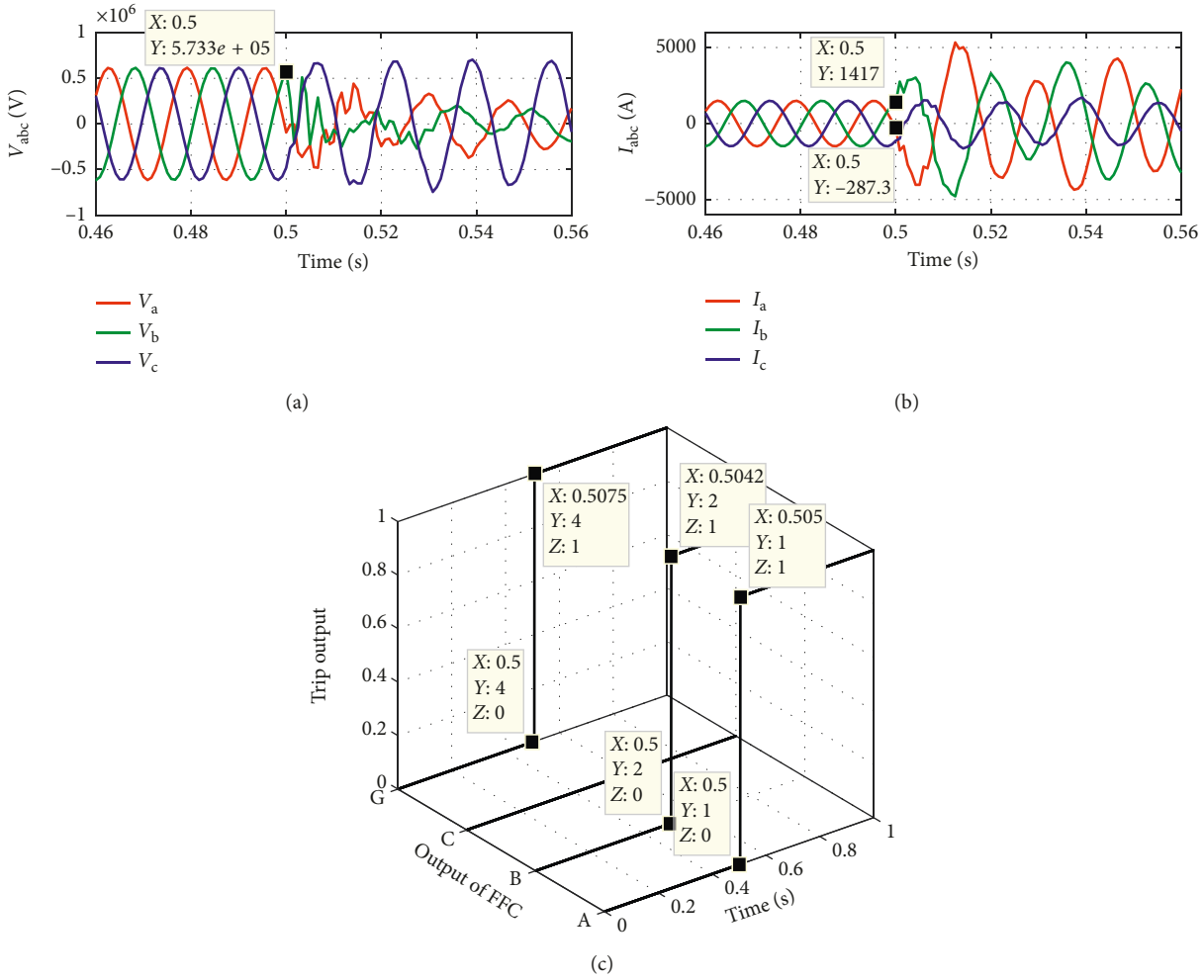

Figure 10: Performance during ABG fault under change in system frequency at 165 km, FIA = 0°, FR = 20 Ω, and f = 61 Hz: (a) 3-phase voltage waveform; (b) 3-phase current waveform; (c) output of FFC.

Table 11: Simulation results for the heavy load interconnection (FIA = 0° and FL = 165 km).

Simulated system data			Results obtained from the proposed CDFTF-based scheme				
Load		Switching instant (s)	Response time (ms)				Fault type
P (in MW)	Q (in MVAr)		Phase A	Phase B	Phase C	Ground G	
500	300	0.5	0	0	0	0	No fault
800	600		0	0	0	0	No fault
1000	800		0	0	0	0	No fault

Consider the load of P = 1000 MW and Q = 800 MVAr is inserted on bus B2 in Figure 1, and the switching instant of load to bus B2 is 0.5 sec at the system frequency of 60 Hz. Fault classification outputs during this heavy load interconnection are shown in Figures 11(a) and 11(b), respectively. Figures 11(a) and 11(b) show 3-phase voltage and current waveform, and Figure 11(c) presents the output of FFC wherein all the phases, i.e. A, B, and C, and ground G is low (0) all the time. The results approve that performance of the proposed scheme is perfect with varying system frequency.

5. Validation of the Proposed Scheme Using EMTDC/PSCAD

In order to test the proposed CDFTF-based scheme with more realistic system conditions, different fault situations have been simulated in the modified WSCC 3-machine 9-bus system [26] using EMTDC/PSCAD software. The system parameters are given in Appendix B. The single-line diagram of the modified WSCC 9-bus system is shown in Figure 12. The relay is placed near to bus 7, so the transmission line

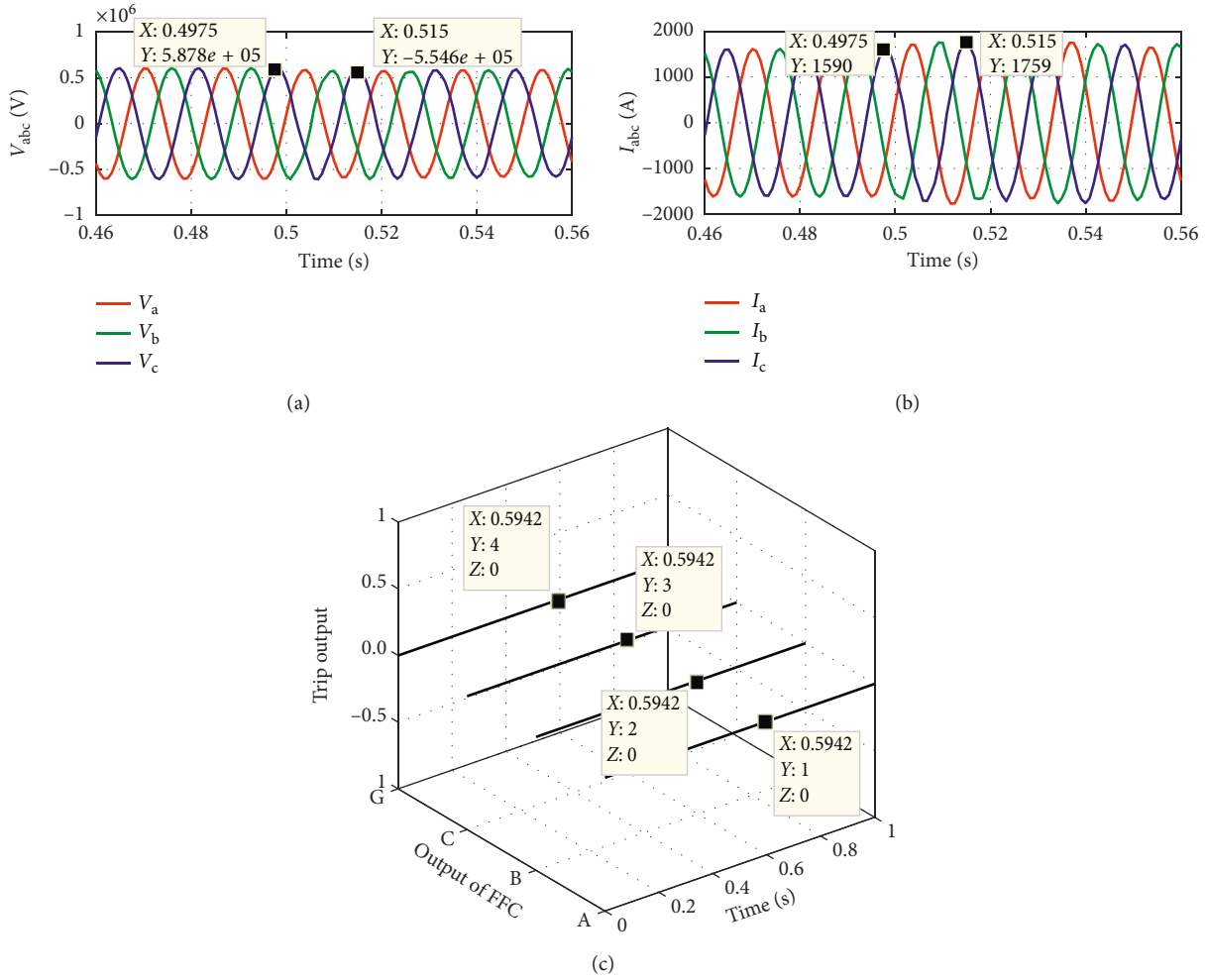

FIGURE 11: Performance during heavy load condition at 300 km, $P = 1000$ MW, and $Q = 800$ MVAr: (a) 3-phase voltage waveform; (b) 3-phase current waveform; (c) output of FFC.

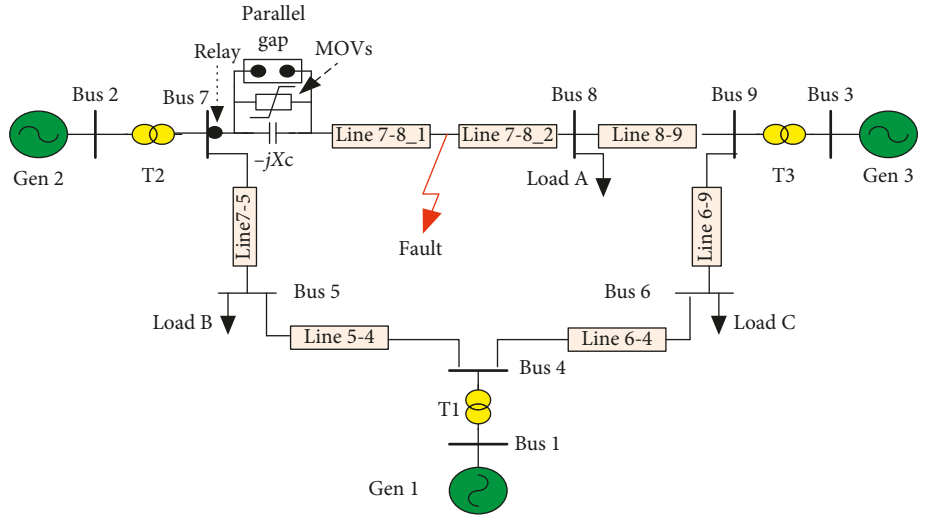

FIGURE 12: Single-line diagram of the modified WSCC 3-machine 9-bus system.

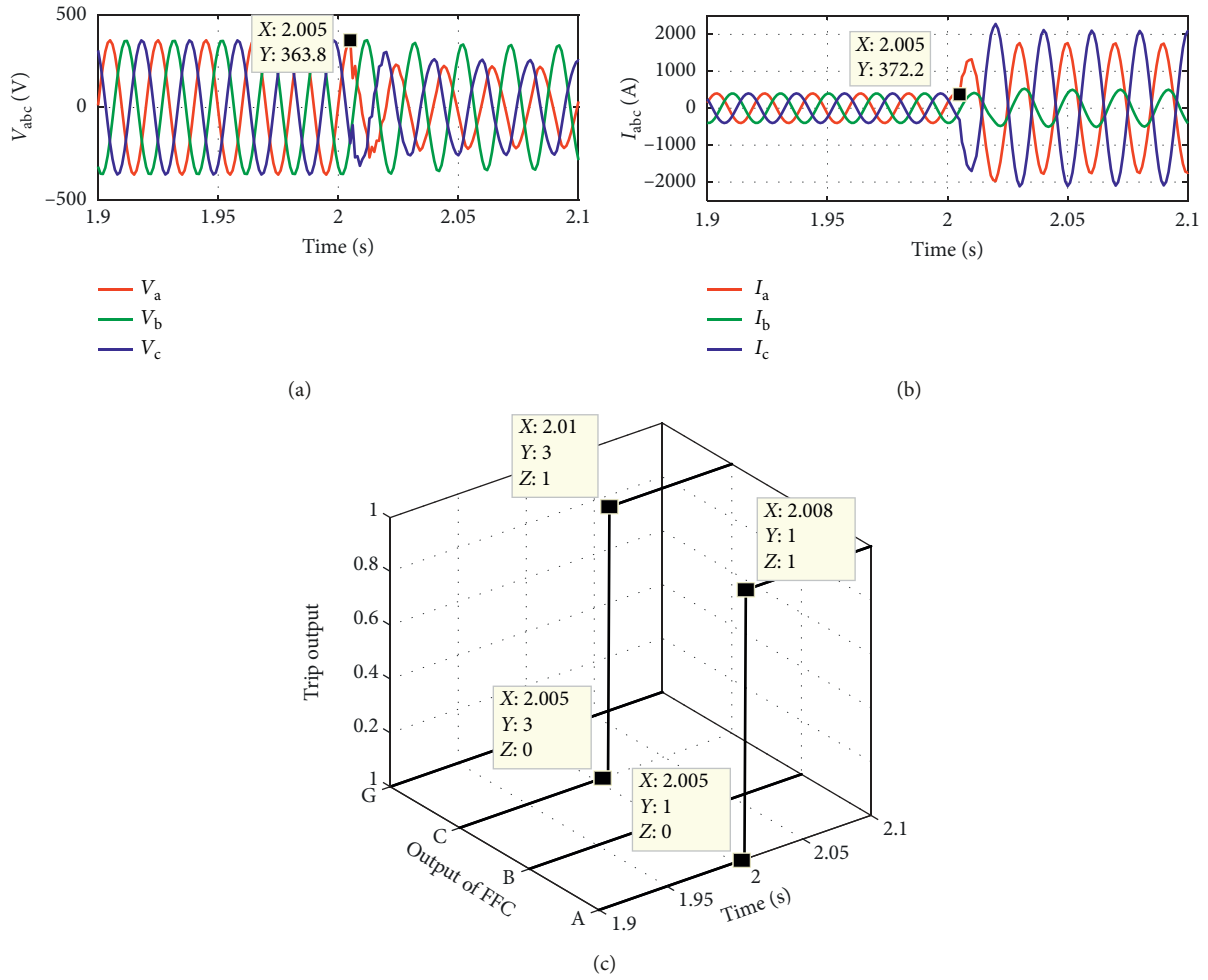

FIGURE 13: Performance during CA fault at 160 km, FIA = 90°, FR = 0.001 Ω, and %Xc = 40%: (a) 3-phase voltage waveform; (b) 3-phase current waveform; (c) output of FFC.

between bus 7 and bus 8 is considered to be protected which is 40% series compensated by a fixed series capacitor. Different fault situations have been simulated by varying fault parameters such as fault type (LG, LLG, LL, and LLL), fault location (10–390 km with a step of 10 km), fault inception angle (0°–315° with a step of 45°), and fault resistance (0–100 Ω with a step of 20 Ω). The fault signals generated from PSCAD software are preprocessed using MATLAB/Simulink software to obtain fundamental component values of voltage and current signals and then used as input to the fuzzy logic-based classifier:

$$\text{accuracy}\,(\%) = \frac{\text{number of correctly classified fault cases}}{\text{total number of test cases}} * 100. \quad (2)$$

The fault classification modules correctly identify the involvement of phase(s) and ground. For instance, CA fault is created at 160 km, FIA = 90°, FR = 0.001 Ω, and %Xc = 40%; in this case, the three-phase voltage and current signals obtained from PSCAD software simulation are shown in Figures 13(a) and 13(b), and output of the fuzzy fault classifier is shown in Figure 13(c). Figure 13(c) shows the performance of the classification module in which phases A and C rise up (1) both at 3 ms and 5 ms, respectively, while phase B and ground G remain low (0) after the inception of the fault at 2.005 sec. Some of the test results are presented in Table 12. Analyzing the results of Table 12, it is concluded that the proposed method has an accurate and reliable performance in various system conditions in the modified WSCC 3-machine 9-bus system.

For investigating the robustness of the proposed scheme, different faults are simulated in different conditions by varying different fault parameters. Total fault cases simulated are 5 (RF value) × 32 (fault locations) × 8 (FIA) × 10 (fault type) + 20 = 12820 cases. All these test cases have been applied to the proposed scheme, and the fault classification accuracy and correctness are measured in terms of the confusion matrix and presented in Table 13. The confusion matrix is a very concrete method to measure of robustness and accuracy of the proposed scheme. It can be observed from the confusion matrix that all the cases are predicted by the proposed scheme with an average accuracy of 99.678%. The result confirms that the proposed CDFTF-based scheme works correctly for the EMTDC/PSCAD fault simulation also.

Table 12: Effect of fault resistance, fault inception angle, and fault location.

Simulated system data				Results obtained from the proposed CDFTF-based scheme				
				Response time (ms)				
FL (km)	Fault type	FR (ohm)	FIA (degree)	Phase A	Phase B	Phase C	Ground G	Fault type
	CG	100	0	—	—	8	3	CG
20	ABG	80	90	5	7	—	2	ABG
	ABC	20	225	3.5	4.5	5.5	—	ABC
	CAG	0.001	45	4.5	—	6.5	2.5	CAG
120	AG	40	90	6	—	—	4	AG
	AB	60	135	9.5	7.5	—	—	AB
	AC	0.001	90	3	—	4	—	AC
160	BG	60	180	—	6	—	4	BG
	BCG	100	45	—	10.5	7.5	3.5	BCG
	CG	0.001	0	—	—	11	4	CG
240	BC	80	45	—	10.5	12.5	—	BC
	ABC	100	90	12	10	7	—	ABC
	AG	20	135	11.5	—	—	8.5	AG
290	AC	40	180	18	—	10	—	AC
	ABG	0.001	45	5.5	12.5	—	6.5	ABG

Table 13: Confusion matrix for the CDFTF-based scheme.

Actual fault														
Predicted fault	Sample	AG	BG	CG	AB	BC	CA	ABG	BCG	CAG	ABC	No fault	Accuracy (%)	Average accuracy (%)
AG	1280	1276	0	0	0	0	0	0	0	0	0	4	99.68	
BG	1280	0	1272	0	0	0	0	0	0	0	0	8	99.37	
CG	1280	0	0	1280	0	0	0	0	0	0	0	0	100	
AB	1280	0	0	0	1278	0	0	2	0	0	0	0	99.84	
BC	1280	0	0	0	0	1277	0	0	2	0	0	1	99.76	
CA	1280	0	0	0	0	0	1280	0	0	0	0	0	100	**99.678**
ABG	1280	0	0	0	12	0	0	1268	0	0	0	0	99.06	
BCG	1280	0	0	0	0	16	0	0	1264	0	0	0	98.75	
CAG	1280	0	0	0	0	0	0	0	0	1280	0	0	100	
ABC	1280	0	0	0	0	0	0	0	0	0	1280	0	100	
No fault	20	0	0	0	0	0	0	0	0	0	0	20	100	

Table 14: Comparisons with other schemes.

Parameter	Proposed algorithm	Reference [7]	Reference [8]	Reference [10]	Reference [13]
Time to classify fault	Half or less than one cycle	Half cycle	Half cycle	Not reported	Not reported
Input signals used	3-phase single-ended voltage and current	3-phase current samples	3-phase current samples	3-phase voltage and current	3-phase current samples
Algorithm used	Combined DFT and fuzzy logic	Integrated moving sum approach	Wavelet transform and ChNN	Wavelet transform and fuzzy nuerosystem	Support vector machine
Number of test cases	129600	Not mentioned	54000	23436	25200
Fault resistance	0.001 Ω–100 Ω	10 Ω, 50 Ω, and 150 Ω	0 Ω, 5 Ω, 25 Ω, and 50 Ω	0.1 Ω, 5 Ω, 25 Ω, and 50 Ω	0 Ω, 5 Ω, 25 Ω, and 50 Ω
Fault inception	0°–360°	54° and 90°	0°, 45°, 80°, and 115°	0°, 45°, and 90°	0°, 45°, and 115°
Evolving fault considered	Yes	Not reported	Not reported	Not reported	Not reported
Compensation level	10–65%	70%	25, 50, and 75%	20, 40 and 60%	25, 50 and 75%
Change in frequency	58 Hz–62 Hz	Not reported	Not reported	Not reported	Not reported
Heavy load interconnection	Yes	Not reported	Not reported	Not reported	Not reported

6. Comparisons with Other Schemes

A summarized result of the comparative performance evaluation of the proposed CDFTF-based scheme with some other classification methods available in the literature is shown in Table 14. Most of the schemes reported in Table 14 have not discussed regarding the evolving fault, change in the system frequency, and heavy load interconnection. In most of the cases, the proposed schemes take half cycle time to classify the faults and the accuracy is about 100% compared to all other methods shown in Table 14. It can be observed that the time required by the proposed CDFTF-based scheme to classify the fault is 1/2–1 cycle. In addition, the proposed scheme is robust to wide variations in fault parameters, and moreover the scheme works well for evolving fault classification also. Furthermore, the performance is not affected by change in frequency and heavy load interconnection which have not been considered by earlier reported techniques.

7. Conclusion

This article presents a combined discrete Fourier transform and fuzzy logic based relaying scheme for protection of the series compensated transmission line. The process is started at retrieving the current and voltage signal features and preprocessing through discrete Fourier transform to obtain the fundamental component of voltage and current. The voltage and current features are used to build the fuzzy rule base for detection and classification of faults. The speed of the presented relaying technique is within half cycle of power frequency. Regarding fault detection and classification, the algorithm is capable of detecting and classifying all types of faults under varying fault and system conditions. Also, the variation in fault location, fault resistance, system frequency, and evolving fault do not affect the classification process. The CDFTF-based fault classification scheme has proved to be reliable, fast, and accurate against different fault situations in different series compensated transmission systems.

Appendix

A. System Parameter Details of Network Shown in Figure 1

The parameters of each line are as follows:
Line 1: 100 km
Line 2: 300 km
Positive sequence impedance = $0.01273 + j0.35199\ \Omega$/km
Positive sequence capacitance = $0.01274\ \mu$F/km
Zero-sequence impedance = $0.3864 + j1.5556\ \Omega$/km
Zero-sequence capacitance = $0.007751\ \mu$F/km
Compensation level: 40%
MOV voltage rating: 298.7 kV, 30 MJ
Parameters of each source are as follows:
Source 1: $6 * 350$ MVA, 13.8 kV, 60 Hz, $\%X = 22$
Source 2: 30000 MVA, 735 kV, 60 Hz
Parameters of each transformer are as follows:
Transformer 1: 350 MVA, 13.8/735 kV, 60 HZ, $\%X = 8\%$
Transformer 2: 300 MVA, 735/230 kV, 60 Hz, $\%X = 15\%$
Parameters of each load are as follows:
Load 1: $P = 100$ MW
Load 2: $P = 132$ MW, $Q = 330$ MVAr
Load 3: $P = 132$ MW, $Q = 330$ MVAr
Load 4: $P = 250$ MW

B. System Parameter Details of Network Shown in Figure 12

System data for WSCC 3-machine 9-bus configuration:
Generator:
Gen 1: 600 MVA, 22 kV, 50 Hz; Gen 2: 465 MVA, 22 kV, 50 Hz; Gen 3: 310 MVA, 22 kV, 50 Hz
$X_d = 1.81$ p.u., $X'_d = 0.3$ p.u., $X''_d = 0.23$ p.u., $T'_{d0} = 8$ s, $T''_{d0} = 0.03$ s, $X_q = 1.76$ p.u., $X''_q = 0.25$ p.u., $T''_{q0} = 0.03$ s., $R_a = 0.003$ p.u., X_p (Potier reactance) = 0.15 p.u.
Transformer:
T1: 600 MVA, 22/400 kV, 50 Hz, /Y
T2: 465 MVA, 22/400 kV, 50 Hz, /Y
T3: 310 MVA, 22/400 kV, 50 Hz, /Y
$X = 0.163$ p.u., $X_{core} = 0.33$ p.u., $R_{core} = 0.0$ p.u., $P_{copper} = 0.00177$ p.u.
Transmission line:
Length of line 7-8 = 320 km, line 8-9 = 400 km, line 7-5 = 310 km, line 5-4 = 350 km, line 6-4 = 350 km, line 6–9 = 300 km
Positive sequence impedance = $0.12 + j0.88\ \Omega$/km
Zero-sequence impedance = $0.309 + j\ 1.297\ \Omega$/km
Positive capacitive reactance = $487.723 \times 10^3\ \Omega$/km
Zero-sequence capacitive reactance = $419.34 \times 10^3\ \Omega$/km
Loads:
Load $A = 300$ MW $+ j\ 100$ MVAr
Load $B = 200$ MW $+ j\ 75$ MVAr
Load $C = 150$ MW $+ j\ 75$ MVAr

Data Availability

The data used to support the findings of this study are available from the corresponding author upon request.

Conflicts of Interest

The authors declare that they have no conflicts of interest.

References

[1] B. Vyas, R. P. Maheshwari, and B. Das, "Protection of series compensated transmission line: issues and state of art," *Electric Power Systems Research*, vol. 107, no. 1, pp. 93–108, 2014.
[2] P. M. Anderson, *Power System Protection*, IEEE Press, New York, NY, USA, 1999.
[3] A. G. Phadke and J. S. Thorp, *Computer Relaying for Power Systems*, John Wiley & Sons, Chichester, UK, 1988.
[4] T. Adu, "An accurate fault classification technique for power system monitoring devices," *IEEE Transactions on Power Delivery*, vol. 17, no. 3, pp. 684–690, 2002.
[5] U. B. Parikh, B. R. Bhalja Jr., R. P. Maheshwari, and B. Das, "Decision tree based fault classification scheme for protection of series compensated transmission lines," *International Journal of Emerging Electric Power Systems*, vol. 8, no. 6, 2007.

[6] D. W. P. Thomas, M. S. Jones, and C. Christopoulos, "Phase selection based on superimposed components," *IEE Proceedings-Generation, Transmission and Distribution*, vol. 143, no. 3, pp. 295–299, 1996.

[7] M. Biswal, "Faulty phase selection for transmission line using integrated moving sum approach," *IET Science, Measurement & Technology*, vol. 10, no. 7, pp. 761–767, 2016.

[8] B. Y. Vyas, B. Das, and R. P. Maheshwari, "Improved fault classification in series compensated transmission line: comparative evaluation of Chebyshev neural network training algorithms," *IEEE Transactions on Neural Networks and Learning Systems*, vol. 27, no. 8, pp. 1631–1642, 2016.

[9] J. Upendar, C. P. Gupta, G. K. Singh, and G. Ramakrishna, "PSO and ANN-based fault classification for protective relaying," *IET Generation, Transmission & Distribution*, vol. 4, no. 10, pp. 1197–1212, 2010.

[10] H. Eristi, "Fault diagnosis system for series compensated transmission line based on wavelet transform and adaptive neuro-fuzzy inference system," *Measurement*, vol. 46, no. 1, pp. 393–401, 2013.

[11] P. K. Dash, A. K. Pradhan, and G. Panda, "A novel fuzzy neural network based distance relaying scheme," *IEEE Transactions on Power Delivery*, vol. 15, no. 3, pp. 902–907, 2000.

[12] P. K. Dash, S. R. Samantaray, and G. Panda, "Fault classification and section identification of an advanced series-compensated transmission line using support vector machine," *IEEE Transactions on Power Delivery*, vol. 22, no. 1, pp. 67–73, 2007.

[13] U. B. Parikh, B. Das, and R. Maheshwari, "Fault classification technique for series compensated transmission line using support vector machine," *International Journal of Electrical Power & Energy Systems*, vol. 32, no. 6, pp. 629–636, 2010.

[14] U. B. Parikh, B. Biswarup Das, and R. P. Prakash Maheshwari, "Combined wavelet-SVM technique for fault zone detection in a series compensated transmission line," *IEEE Transactions on Power Delivery*, vol. 23, no. 4, pp. 1789–1794, 2008.

[15] A. Yadav and A. Swetapadma, "Enhancing the performance of transmission line directional relaying, fault classification and fault location schemes using fuzzy inference system," *IET Generation, Transmission & Distribution*, vol. 9, no. 6, pp. 580–591, 2015.

[16] A. K. Pradhan, A. Routray, S. Pati, and D. K. Pradhan, "Wavelet fuzzy combined approach for fault classification of a series-compensated transmission line," *IEEE Transactions on Power Delivery*, vol. 19, no. 4, pp. 1612–1618, 2004.

[17] A. K. Pradhan, A. Routray, and B. Biswal, "Higher order statistics-fuzzy integrated scheme for fault classification of a series-compensated transmission line," *IEEE Transactions on Power Delivery*, vol. 19, no. 2, pp. 891–893, 2004.

[18] B. Das and J. V. Reddy, "Fuzzy-logic-based fault classification scheme for digital distance protection," *IEEE Transactions on Power Delivery*, vol. 20, no. 2, pp. 609–616, 2005.

[19] S. R. Samantaray and P. K. Dash, "Pattern recognition based digital relaying for advanced series compensated line," *International Journal of Electrical Power & Energy Systems*, vol. 30, no. 2, pp. 102–112, 2008.

[20] V. Malathi, N. S. Marimuthu, S. Baskar, and K. Ramar, "Application of extreme learning machine for series compensated transmission line protection," *Engineering Applications of Artificial Intelligence*, vol. 24, no. 5, pp. 880–887, 2011.

[21] A. Swetapadma and A. Yadav, "All shunt fault location including cross-country and evolving faults in transmission lines without fault type classification," *Electric Power Systems Research*, vol. 123, pp. 1–12, 2015.

[22] Z. Moravej, M. Khederzadeh, and M. Pazoki, "New combined method for fault detection, classification, and location in series-compensated transmission line," *Electric Power Components and Systems*, vol. 40, no. 9, pp. 1050–1071, 2012.

[23] M. K. Jena and S. R. Samantaray, "Intelligent relaying scheme for series-compensated double circuit lines using phase angle of differential impedance," *International Journal of Electrical Power & Energy Systems*, vol. 70, pp. 17–26, 2015.

[24] A. Swetapadma, P. Mishra, A. Yadav, and A. Y. Abdelaziz, "A non-unit protection scheme for double circuit series capacitor compensated transmission lines," *Electric Power Systems Research*, vol. 148, pp. 311–325, 2017.

[25] MATLAB, *Version R2013a*, The MathWorks Inc., Natick, MA, USA.

[26] P. K. Nayak, A. K. Pradhan, and P. Bajpai, "A fault detection technique for the series-compensated line during power swing," *IEEE Transactions on Power Delivery*, vol. 28, no. 2, pp. 714–722, 2013.